AIR MOVEMENT & VENTILATION CONTROL WITHIN BUILDINGS

12th AIVC Conference, Ottawa, Canada
24-27 September, 1991

PAPER 2

EVALUATION OF MEASURED AND COMPUTED TEST CASE RESULTS FROM ANNEX 20, SUBTASK 1

G E Whittle
Arup Research and Development
13 Fitzroy Street
London W1P 6BQ
UK

1. INTRODUCTION

The ability to accurately predict air movement and temperature distribution in spaces offers the potential for design engineers to evaluate and optimise room air distribution systems at an early stage, leading to improved thermal comfort and ventilation effectiveness. The computer models which are used for detailed analyses are based on computational fluid dynamics [1,2] and employ sophisticated numerical algorithms to satisfy the basic laws of physics. The programs are such that they are more complex and more difficult to use than those with which design engineers may be more familiar. Specialised skills are required to get the best from the codes, and, as with most new techniques, a greater confidence is needed before their use can be expected to become more routine. It is the latter point concerning confidence in use which is addressed by IEA Annex 20, Subtask 1.

IEA Annex 20 is a task-sharing project on "Air flow patterns within buildings". The objective is to evaluate the performance of single- and multi-zone air and contaminant flow simulation techniques and to establish their viability as design tools. In subtask 1 of the Annex, which deals with single-zone spaces, laboratory experiments in similar test rooms and computer simulations have been carried out at a number of sites in Europe and North America. The data comprises information on air flow patterns and on point-by-point values of mean velocity, turbulent velocity, temperature and contaminant concentration throughout a space.

This paper outlines an initial evaluation of this data and highlights some of the features which the comparisons of measured and computed room air distribution have yielded. Work is continuing in completing the evaluation for tests and data not reported or discussed here.

Besides giving a unified perspective on data from different sites to quantify the general degree of agreement, the evaluation exercise also has the potential for:

- establishing benchmarks for the validation and evaluation of computer codes for room air movement;
- highlighting advantages/limitations of the methods used;
- assessing overall confidence level in computer simulations;
- indicating accuracy and repeatability of measurements and simulations;
- guiding research on simplified models of air movement and identifying problem areas where attention should be focused.

2. THE TEST CONDITIONS

Four full test configurations and one simulation-only test case have been considered. These comprised forced convection,

isothermal flow (case B) [7]; free convection with a radiator (case D) [8], mixed convection, summer cooling (case E) [9], forced convection with contaminant concentration in an isothermal flow (case F) [10], and a two-dimensional isothermal and summer cooling test case (case 2D) [11].

Figures 1 and 2 show the geometry and basic configuration of the basic test room and conditions. The room is sized 4.2m x 3.6m x 2.5m height, with a single-glazed window of area 3.2m^2 in one of the 3.6m walls and a diffuser and extract in the opposite wall [12]. For test case D, a radiator sized 0.3m x 2.0m and rated at 0.862kW was used sited beneath the window [13]. In reality, because existing test facilities were used, some small differences existed in the dimensions of individual test rooms [12].

The supply air diffuser for test cases B and E was the Hesco type KS (no. KS4W205K370) (Figure 3) and was common between all the test facilities [14]. With its 84 tiny nozzles, this type of diffuser provides a real challenge to simulation codes and practitioners.

The two-dimensional test case (isothermal and summer cooling) is shown in Figure 4. The room is specified by ratios of L/H= 3, h/H= 0.056, t/H= 0.16, where 'L' is the room length, 'h' the inlet slot height, 't' the exhaust height and H the room height (3.0m). Experimental data for a Reynolds number of 5,000 is available. For the non-isothermal case, the critical factor is the influence of Archimedes number on jet penetration.

For the contaminant concentration, tests are based on test case B but with the addition of a passive contaminant released in the centre of the room.

The test cases are summarised below.

Test case B (isothermal flow)

Test case B represents forced convection (at isothermal conditions) at three different air flow rates.

Case: B1 flowrate: 0.0158m^3/s (1.5 ach^{-1}).

Case: B2 flowrate: 0.0315m^3/s (3.0 ach^{-1}).

Case: B3 flowrate: 0.0630m^3/s (6.0 ach^{-1}).

Test case D (radiator)

Test case D represents free convection with a radiator located beneath a cold window, with three corresponding radiator and window surface temperatures.

Case: D1 radiator surface temperature: 46°C,
window surface temperatures: 10°C.

Case: D2 radiator surface temperature: 55°C
window surface temperature: 5°C

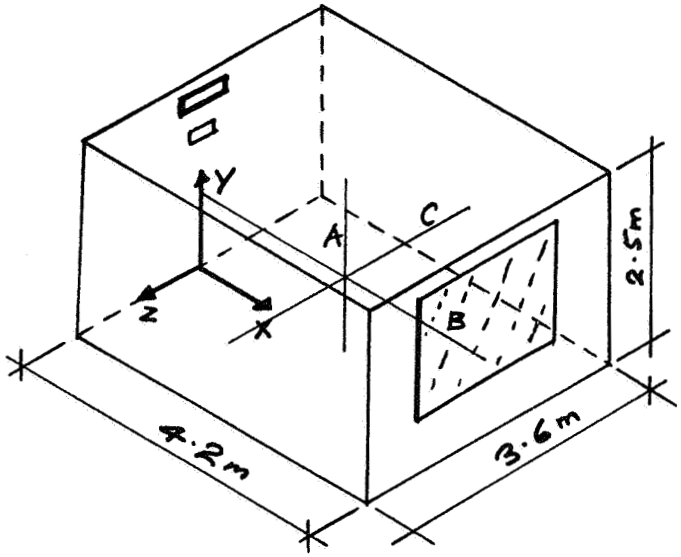

Figure 1. Geometry of test room showing profile locations.

b) Forced convection, isothermal conditions

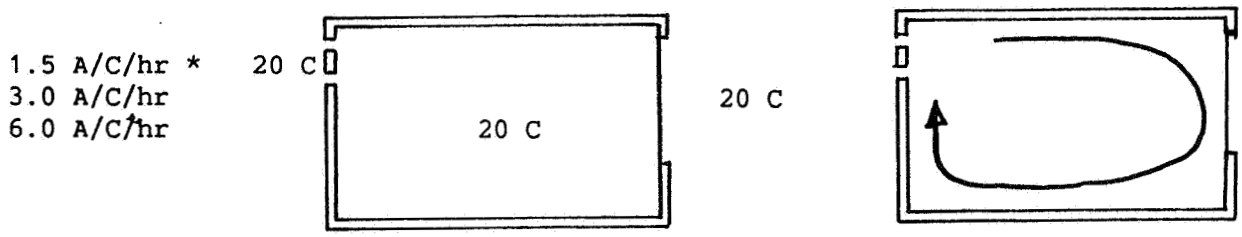

d) Free convection with radiator

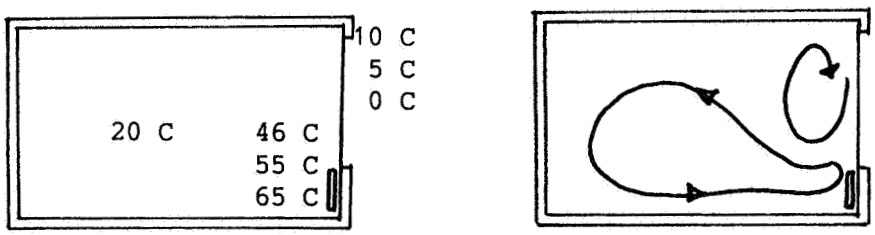

e) Mixed convection, summer cooling

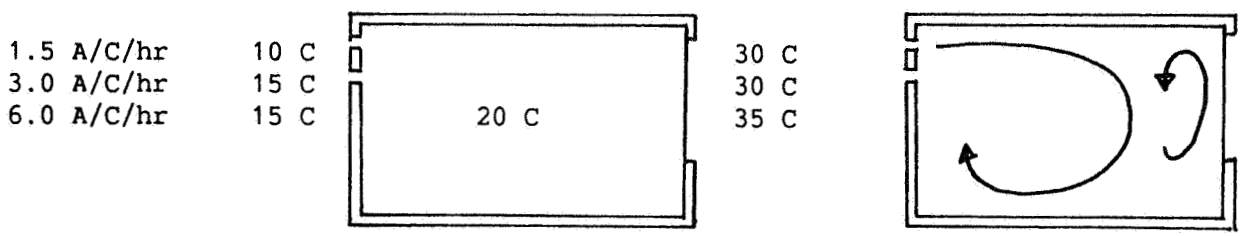

Figure 2 Summary of test case conditions

(* 0.0157, 0.0315, 0.063 m3/s)

Case: D3 radiator surface temperature: 65°C
window surface temperature: 0°C

Test case E (summer cooling)

Test case E represents mixed convection under summer cooling conditions at three different supply air flow rates.

Case: E1 flowrate: 0.0158 m3/s (1.5 ach^{-1}),
supply air temperature: 10°C,
window surface temperature: 30°C.

Case: E2 flowrate: 0.0315 m3/s (3.0 ach^{-1}),
supply air temperature: 15°C,
window surface temperature: 30°C.

Case: E3 flowrate: 0.0630 m3/s (6.0 ach^{-1}),
supply air temperature: 15°C,
window surface temperature: 35°C.)

Test case F (contaminant concentration in isothermal flow)

Test case F represents contaminant concentration in forced convection (at isothermal conditions) at the three different air flow rates indicated above for case B.

Two-dimensional test case 2D (simulation only)

The two-dimensional test case represents both isothermal at a Reynolds number of 5,000, and summer cooling.

3. MEASUREMENTS AND SIMULATIONS

Results were obtained from participants generally according to a prescribed format [15,16]. A full data set for test cases B, D and E comprised 560 points at which mean air speed (Um), turbulent velocity (Ut) and temperature (T) were measured or predicted. In the case of contaminant concentration (case F), then, of course, concentration was also specified. In addition, data on the velocity decay of the supply air jet and the jet penetration length related to Archimedes number were obtained from some participants for test cases B and 2D, and E, respectively.

The specification of 560 points meant that those undertaking simulations were required to limit the data supplied. As expected, simulations were carried out with many thousands of calculation nodes. However, for those undertaking measurements, the requirements of the 560 specified points proved to be demanding. Some contributors concentrated their attention in measuring the detailed flow structure in the jet, whilst others were able to measure throughout the space and mostly, but not universally, at all the agreed positions.

Table 1 identifies the co-ordinates of the standard measuring locations. As a subset of these locations, an occupied zone is defined up to a height of 1.8m and to within 0.6m of walls [3,4].

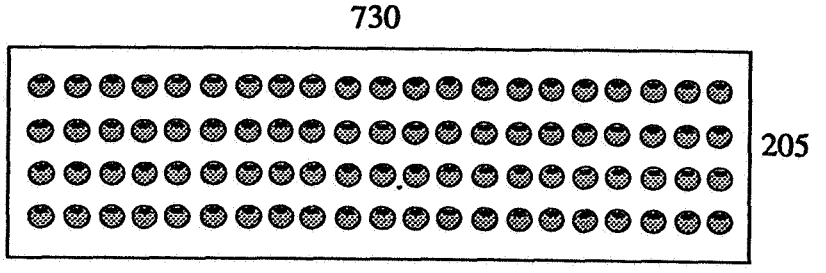

Figure 3 Hesco diffuser (84 nozzles)

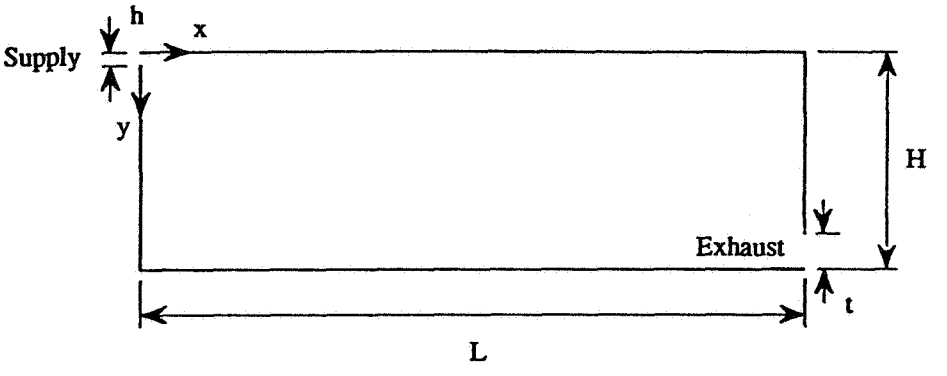

Figure 4 2D Testcase

Table 1 Measurement locations (see Figure 1)

X	Y (height)	Z
0.1	0.05	-1.7
0.6	0.10	-1.2
1.4	0.2	-0.6
2.2	0.5	0.0
3.0	1.0	0.6
3.6	1.5	1.2
4.0	2.0	1.7
4.1	2.3	
	2.4	
	2.45	

Occupied zone data is of interest to designers in assessing thermal comfort and ventilation effectiveness.

The measuring instrumentation was mainly based on thermal anemometry using hot-wire and omnidirectional hot-film probes from Disa-Dantec, TSI and B&K, IMG constant-current hot_wire, and constant-temperature thermistors.

The computer codes used were all of finite volume formulation and all utilised a pressure-correction method [1]. The codes were: CALC-BFC, EOL3D, EXACT3, FLUENT, KAMELEON, PHOENICS, SIMULAR-AIR, WISH3D. A number of zonal models were also used, operated by INSA/CSTB, France.

CFD simulations were carried out with the different codes identified above, with collective guidance given on options for modelling boundary conditions such as the supply terminal [17] and the radiator [18]. For the supply terminal, alternative inlet models were defined. These included a basic model with an opening of 0.180m x 0.062m representing the diffuser, a prescribed velocity model where the velocity is fixed over a surface some distance from the diffuser. The code operators were free to generate meshes which they felt were appropriate, bearing in mind the need to resolve certain features of the flow such as the supply air jet and boundary layers, whilst also recognising practical limitations associated with computing resources, code capabilities and project time-scale. Some contributors investigated different options in specifying boundary conditions, in mesh resolution and alternative differencing schemes. The difference schemes used include Upwind, Hybrid, Power Law and Quick. All CFD simulations were carried out with turbulence represented using the two-equation k - epsilon model. Some turbulence models incorporated the buoyancy-extension to represent the generation or suppression of turbulence energy due to temperature gradient, and some models incorporated a low Reynolds number variant.

Most simulations were carried out in one half of the room, assuming symmetry, although some simulation data was generated for the whole space.

More detailed information on the methods used in these studies can be found in participants' individual reports listed in the References section at the end of this paper.

4. DATA ANALYSIS

The fundamental quantities which are calculated and compared are the mean air speed (Um), turbulent velocity scale (Ut), air temperature (T) and contaminant concentration. However, the mean air speed from measurements using an omni-directional probe is the time-averaged value of velocity, whilst in simulations it is the magnitude of the mean velocity. The turbulent velocity from measurements is the standard deviation of velocity (given by an omnidirectional probe), but in simulations it is $(2k)^{1/2}$ where 'k' is the turbulent kinetic energy per unit mass. These are not identical physical quantities since averaging is performed

differently. To ensure consistency between measurements and simulations [7,19] a modified air speed has been defined, where the modified air speed is,

$$U^* = (Um^2 + Ut^2)^{0.5}$$

This has been presented only for the averaged comfort parameters and for some statistical comparisons. In practice, the modified air speed is very similar to mean air speed, but it relies on two items of data and is more difficult to interpret in a physical sense, and hence has limited value.

Measurement and simulation data are considered in the following ways:

Flow patterns

A comparison of flow patterns provide a first and qualitative indication of whether agreement exists between data sets. Indications are given in the figures of flow patterns and contours of velocity and temperature for selected cases. These are reproduced from participants' reports. In the case of measured data, speed contours are shown rather than vector plots.

Key comfort parameters

The thermal comfort of occupants and air movement in the room can be assessed by consideration of comfort parameters such as average air speed, turbulence, and air temperature, and the maximum and minimum air temperatures in the occupied zone [3,4]. The measured data shown is that for the whole of the occupied zone whilst the simulation data was generated mainly for half the zone (by specifying a symmetry boundary along the middle of the room).

Statistical correlations and RMS differences

Some early analysis was carried out using a statistically-based point-by-point comparison of data using calculations of linear correlation coefficient and RMS error.

The sample linear correlation coefficient (SCC) and root mean square of the difference (RMS) was calculated between each pair of data sets for the modified air speed, the turbulence scale and the air temperature according to the following formulae [5]:

For the SCC between the mean air speeds (Um) predicted by participant A and that of participant B,

$$SCC, Um(A,B) = \frac{n\sum Um_i^{(A)} Um_i^{(B)} - \sum Um_i^{(A)} \sum Um_i^{(B)}}{\sqrt{n\sum Um_i^{(A)^2} - \left(\sum Um_i^{(A)}\right)^2}\sqrt{n\sum Um_i^{(B)^2} - \left(\sum Um_i^{(B)}\right)^2}}$$

where the summation is from i= 1, n over the n (= 560 = 10*8*7)

standard measuring points. e.g. Um_1 is Um for the point X= 0.1, Y= 0.05, Z= 0.0. Similarly the RMS difference between the data sets is given by,

$$RMS, Um(A,B) = \sqrt{\frac{\sum \left(Um_i^{(A)} - Um_i^{(B)}\right)^2}{n}}$$

Thus, the results from participant A are compared with those of participant B for the corresponding measuring points. The SCC must take a value between +1 and -1 with +1 arising if, plotting Um(A) against Um(B), all 560 points lie on a straight line with positive slope. Correspondingly lower values arise when the points show greater scatter about the linear regression line.

RMS values will range upwards from 0 (perfect agreement between all 560 measured and simulated values) and have the units of the variables being compared.

In practice, correlation coefficients and RMS difference were relatively large even comparing measured to measured data. The nature of room air movement, which is characterised by large amplitude and low frequency velocity fluctuations, is such that point-by-point comparisons do not yield meaningful results. Therefore, analyses using this approach has been discontinued.

4.5 Profiles/graphs

Velocity decay with distance from the diffuser, variation of maximum (or mean) velocity in the room and penetration length of the jet in summer cooling have been identified as a critical factors in quantifying agreement. Examples of some of these graphs are shown in this paper.

5. MAIN FINDINGS

Work is continuing from previous analyses [35,36] in comparing and evaluating the data. Some observations are made below.

Test case B (isothermal flow)

Air flow patterns for the isothermal case (B1, B2 and B3) are well predicted by the simulation models. As examples of velocity fields, Figure 5 show air centre-line speed contours for case B2 from measured data from Blomqvist [20] and from Heikkinen [21] compared to simulation data from Skovgaard [22].

Occupied zone data on mean velocity, turbulent velocity, modified velocity and maximum velocity are summarised in Tables 2, 3 and 4.

As seen in Figure 6 the occupied zone velocities increase almost linearly with supply air flow rate, as expected (Tests B1 to B2 to B3). There are, though, simulation results where the predicted

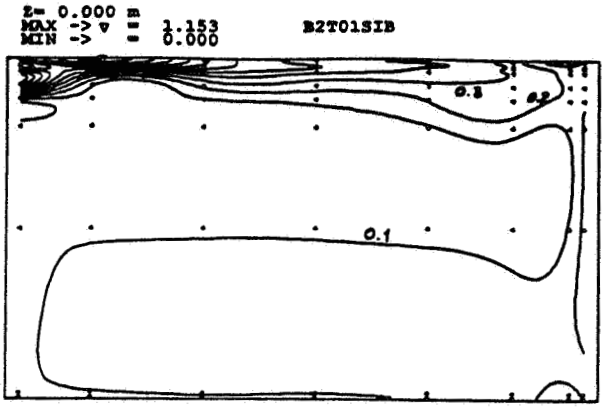

Isovels in plane z= 0.0 m

Measurements from Blomqvist

Case b2, plane 1, measured air speed, m/s

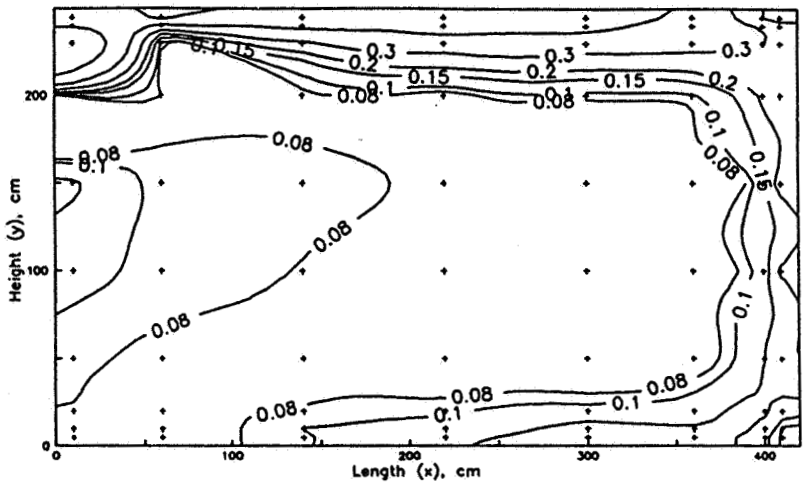

Measurements from Heikkinen

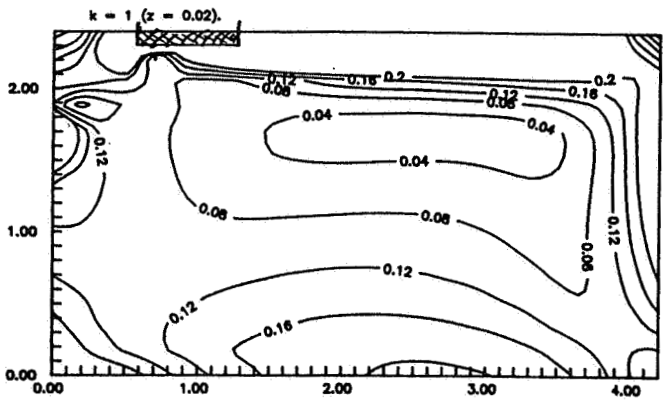

Simulation from Skovgaard

Figure 5 Test case B2

Table 2 Test case B1

Ref.	M or S	Ave. Um	Ave. Ut	Ave. U*	Max Um	Max Temp	Ave. Temp	Min Temp
B1CH	S	0.020	0.007	0.022	0.038	-	-	-
B1_CTH_C	S	0.032	0.010	0.034	0.057	-	-	-
B1C01SF1	S	0.041	0.010	0.043	0.073	-	-	-
B1004DK	S	0.041	0.019	0.046	0.070	-	-	-
B1001DK	S	0.045	0.019	0.051	0.075	-	-	-
B1GER	S	0.049	0.022	0.055	0.090	-	-	-
B1C03SF1	S	0.053	0.014	0.055	0.093	-	-	-
B1M001NL	M	0.059	-	0.059	0.123	-	-	-
B1P001NL	S	0.060	0.016	0.063	0.104	-	-	-
B1FRG	S	0.083	0.036	0.093	0.151	-	-	-

M= measured, S= simulated

Table 3 Test case B2

Ref.	M or S	Ave. Um	Ave. Ut	Ave. U*	Max Um	Max Temp	Ave. Temp	Min Temp
B2CD	S	0.017	0.005	0.020	0.049	-	-	-
B2N2	S	0.027	0.107	0.114	0.073	-	-	-
B2_CTH-C	S	0.033	0.010	0.035	0.060	-	-	-
B2CH	S	0.048	0.019	0.052	0.086	-	-	-
B2T01SIB	M	0.082	0.031	0.089	0.189	22.30	21.08	20.20
B2FRG	S	0.083	0.036	0.093	0.151	-	-	-
B2C01SF1	S	0.092	0.024	0.097	0.161	-	-	-
B2T03SF1	M	0.100	0.023	0.103	0.178	18.40	18.07	17.75
B2C02SF1	S	0.108	0.029	0.113	0.189	-	-	-
B2C03SF1	S	0.108	0.029	0.113	0.189	-	-	-
B2B002NL	S	0.108	0.022	0.112	0.190	-	-	-
B2B001NL	S	0.109	0.019	0.112	0.192	-	-	-
B2GER	S	0.109	0.047	0.122	0.211	-	-	-
B2C04SF1	S	0.119	0.040	0.128	0.205	-	-	-
B2P001NL	S	0.123	0.034	0.129	0.213	-	-	-
B20F	S	0.130	0.055	0.146	0.221	-	-	-
B2004DK	S	0.131	0.054	0.145	0.222	-	-	-
B2P002NL	S	0.135	0.051	0.148	0.234	-	-	-
B2001DK	S	0.151	0.061	0.167	0.252	-	-	-

Table 4 Test case B3

Ref.	M or S	Ave. Um	Ave. Ut	Ave. U*	Max Um	Max Temp	Ave. Temp	Min Temp
B3CH	S	0.033	0.053	0.063	0.070	-	-	-
B3_CTH_C	S	0.034	0.010	0.036	0.061	-	-	-
B3C01SF1	S	0.190	0.052	0.202	0.333	-	-	-
B3T02SF1	M	0.205	0.055	0.213	0.418	18.65	18.40	17.97
B3C03SF1	S	0.218	0.061	0.229	0.381	-	-	-
B3GER	S	0.221	0.095	0.247	0.434	-	-	-
B3FRG	S	0.242	0.092	0.265	0.440	-	-	-
B3P001NL	S	0.251	0.070	0.264	0.436	-	-	-
B3004DK	S	0.253	0.104	0.280	0.428	-	-	-
B3001DK	S	0.314	0.123	0.347	0.527	-	-	-

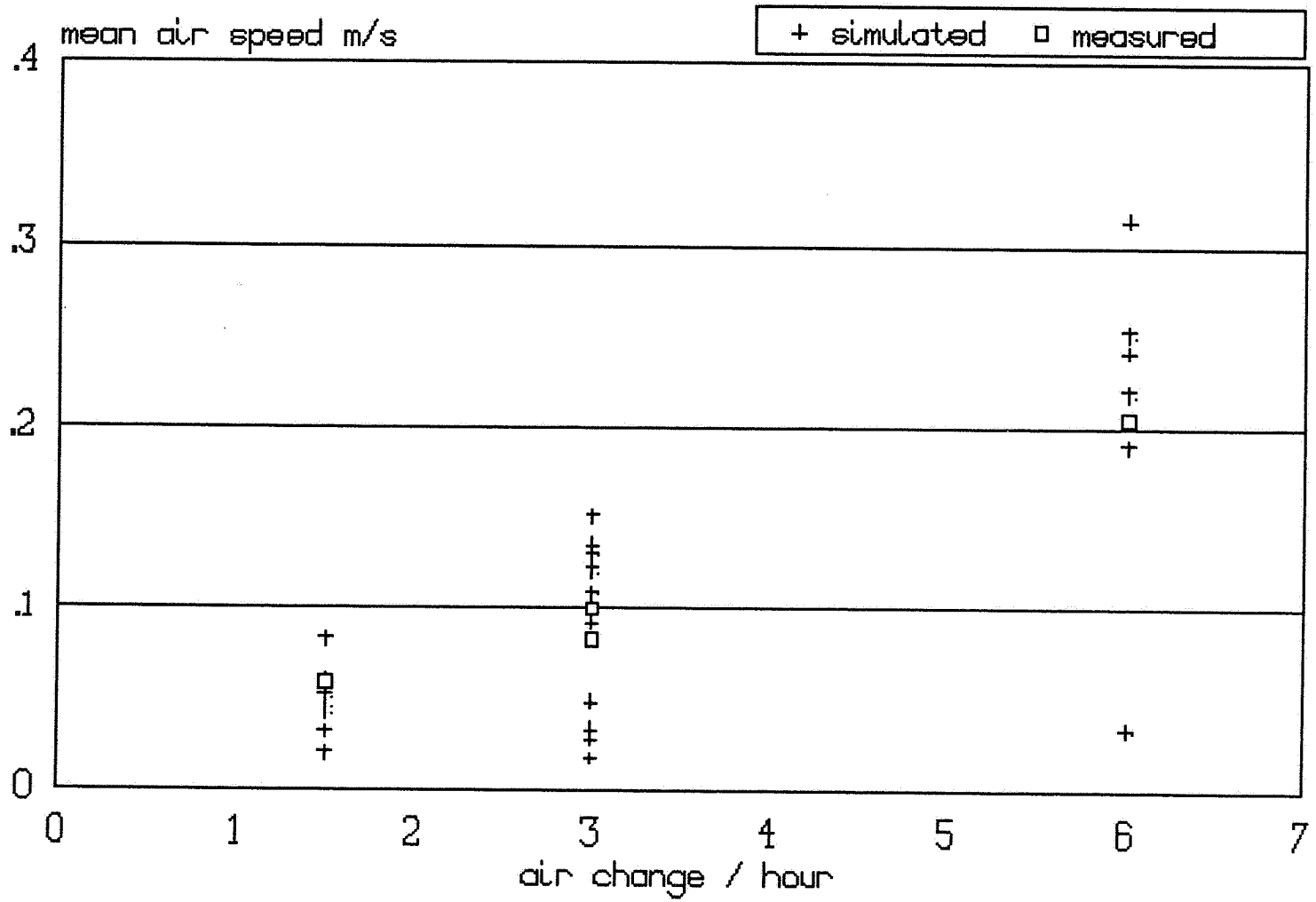

Figure 6 Occupied zone air speed (test cases B)

mean velocity is clearly too low and some which are high. It is unclear as yet whether this is due to the characteristics of the code used or related to assumptions made by the operator. The figures for modified velocity generally follow those for the mean velocity.

It should be noted that certainly for case B1 and possibly case B2 the mean velocities are very low and hence difficult to measure with any reasonable accuracy.

In reality it may be expected that some low Reynolds number effects would be evident at the low flow rate end of the range. However, those who performed simulations using a high Reynolds number turbulence model (the majority) would not expect to predict this. Individual researchers have commented on measurements [6] and have discussed the physical effects and models [23,24].

Regarding numerics, Vogl and Renz [25] indicated that the Quick differencing scheme on a fine grid had the potential for a greater accuracy, although the scheme exhibited poorer numerical stability than the power law scheme.

Test case D (natural convection, radiator)

Figures 7 and 8 show speed and temperature contours from measurements (Lemaire [29]) and simulation (Heikkinen and Piira [30]) of case D2, and Tables 5-7 summarise the occupied zone velocity and temperature data.

The air velocities in the occupied zone are uniformly low, and the average temperature is in almost all cases between 20°C and 21°C. It is unfortunate that measured data is limited, and that the only set indicates an occupied zone air speed higher than the simulation data and a temperature slightly lower.

In simulations, Lemaire [26] found that the flow pattern remained similar for the three cases, with the pattern driven by the buoyant flow from the radiator upwards over the cold window. Prescribed heat fluxes were used for the radiator and the window. Previous simulations had demonstrated that the logarithmic wall functions dramatically under-predict the surface convection coefficients.

Zonal model results have been generated by Inard and Buty [27] for comparison with measurements and CFD simulations. It is found for case D2 and for assumed constant heat transfer coefficients, that a single-zone model yields the same mean air temperature of 20.3°C as a five-zone model. However, a similar two-zone model gives an increase in mean temperature of about 0.6°C, whilst the assumption of variable convection coefficients in a five-zone model reduces the mean air temperature by approximately 0.6°C. The predicted temperature gradients vary from 0.4°C (five-zone, variable convection coefficients) to 1.2°C (two-zone, constant convection coefficients). Similar findings apply for cases D1 and D3.

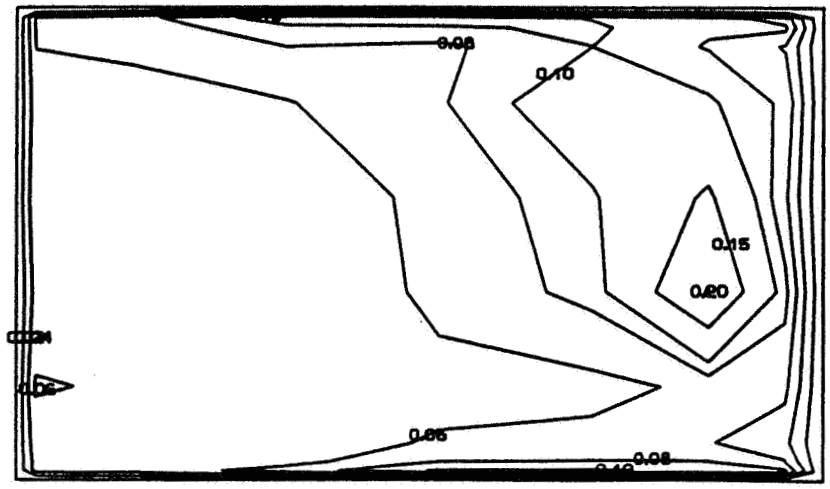

Run: d2M001NL
Iso-vels (m/s)
plane k = 1
(z = 0.00 m)

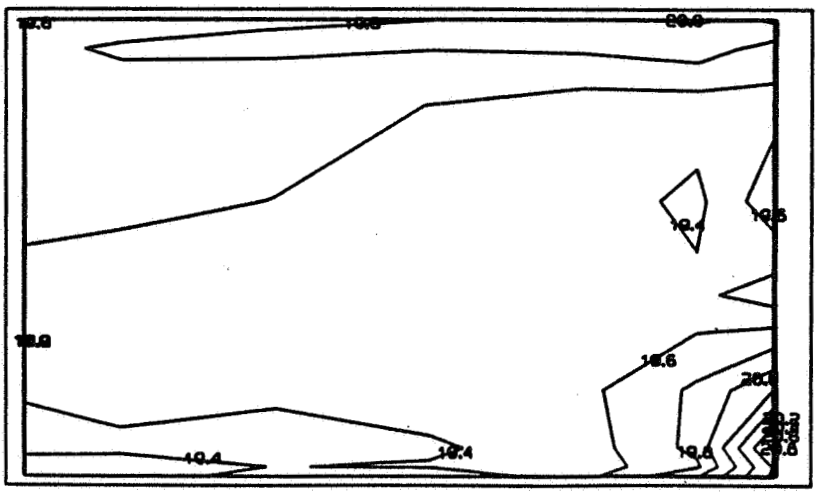

Run: d2M001NL
Isotherms (°C)
plane k = 1
(z = 0.00 m)

Figure 7 Measurement data for test case D2
(from Lemaire)

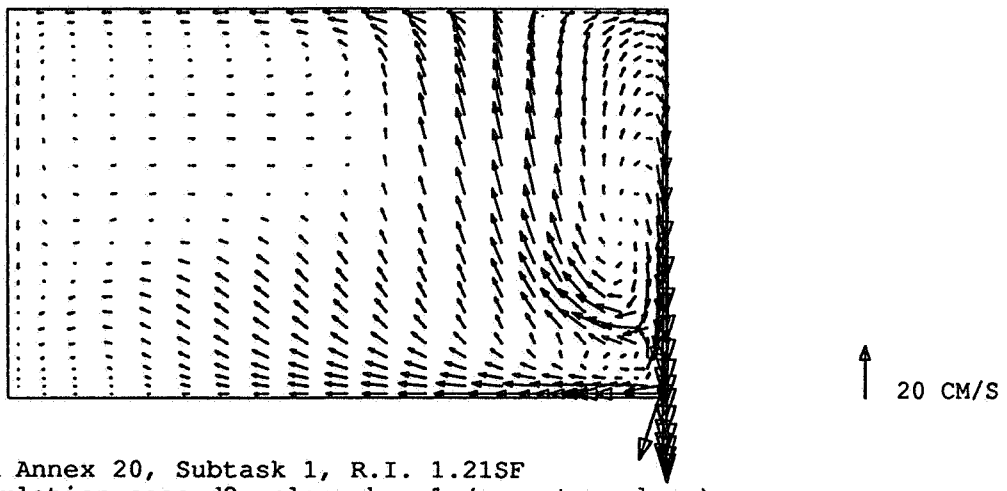

IEA Annex 20, Subtask 1, R.I. 1.21SF
Simulation case d2, plane k = 1 (symmetry plane)
Simulated velocity vectors

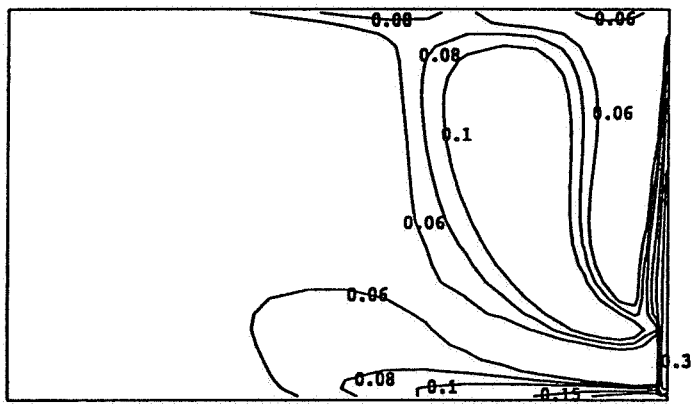

IEA Annex 20, Subtask 1, R.I. 1.21SF
Simulation case d2, plane k = 1 (symmetry plane)
Simulated contours of velocity (m/s)

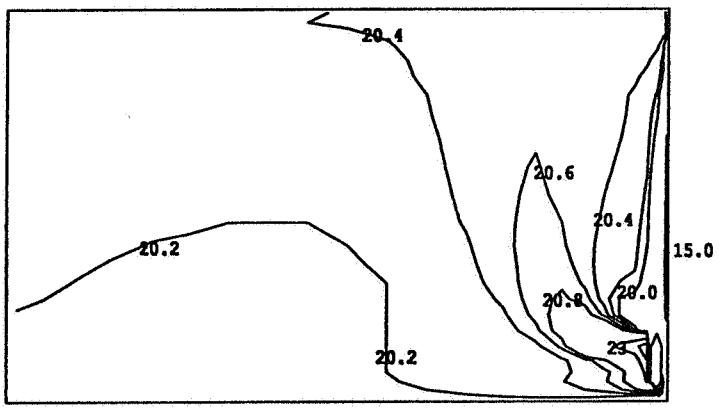

IEA Annex 20, Subtask 1, R.I. 1.21SF
Simulation case d2, plane k = 1 (symmetry plane)
Simulated contours of temperature (^{o}C)

Figure 8 Simulation data for test case D2 (from Heikkinen)

Table 5 Test case D1

Ref.	M or S	Ave. Um	Ave. Ut	Ave. U*	Max Um	Max Temp	Ave. Temp	Min Temp
D1CH	S	0.017	0.009	0.020	0.074	20.54	20.28	20.08
D1Q001NL	S	0.020	0.005	0.021	0.081	20.89	20.40	20.06
D1FRG	S	0.022	0.014	0.028	0.046	21.10	20.52	20.10
D11GER	S	0.028	0.007	0.030	0.085	21.76	20.93	20.23
D1CO2SF1	S	0.036	0.020	0.042	0.127	20.66	20.15	19.89
D1GER	S	0.037	0.019	0.042	0.126	20.38	20.11	20.01

M= measured, S= simulated

Table 6 Test case D2

Ref.	M or S	Ave. Um	Ave. Ut	Ave. U*	Max Um	Max Temp	Ave. Temp	Min Temp
D2CH	S	0.021	0.010	0.025	0.084	20.57	20.29	20.07
D2Q001NL	S	0.022	0.006	0.024	0.087	21.17	20.58	20.11
D2FRG	S	0.024	0.016	0.030	0.049	21.30	20.61	20.10
D2CO1SF1	S	0.026	0.012	0.029	0.154	20.58	20.18	19.98
D21GER	S	0.029	0.008	0.031	0.085	21.56	20.85	20.23
D2CO2SF1	S	0.041	0.022	0.047	0.150	21.06	20.20	19.96
D2GER	S	0.062	0.036	0.074	0.213	20.28	20.10	19.93
D2M001NL	M	0.071	-	0.071	0.203	20.16	19.52	19.23

Table 7 Test case D3

Ref.	M or S	Ave. Um	Ave. Ut	Ave. U*	Max Um	Max Temp	Ave. Temp	Min Temp
D3CH	S	0.019	0.008	0.021	0.085	20.76	20.38	20.09
D3Q001NL	S	0.024	0.006	0.025	0.090	21.57	20.84	20.21
D3FRG	S	0.028	0.018	0.035	0.059	21.60	20.83	20.10
D31GER	S	0.033	0.009	0.035	0.093	21.95	21.12	20.32
D3CO2SF1	S	0.047	0.026	0.055	0.165	20.71	20.23	19.88
D3GER	S	0.058	0.033	0.070	0.227	20.40	20.11	19.91

Test case E (mixed convection, summer cooling)

Figures 9 (Fossdal [32]) and 10 (Blomqvist [33]) show measured speed and temperature contours for case E2. Simulation data from Heikkinen and Piira [34] is shown in Figure 11. The simulation of the jet indicates a slightly earlier and more positive detachment from the ceiling. Table 8-10 summarises the occupied zone velocity and temperature data.

The measured data for the summer cooling case indicates the difficulty in reproducing the test conditions accurately. Figure 12 shows, as expected, a sensitivity of the penetration length of the jet to the Archimedes number for measurement data sets (Blomqvist [28] and Heikkinen [21]) and simulation (Heikkinen [21] and Renz [31]). The measured data from Heikkinen indicates a varying jet penetration length across the room. This test case represents a particularly onerous one to simulate. However, whilst some differences exist between the simulated results and measurement at high Archimedes number the nature of the flow is quite well represented in terms of flow patterns, mean velocities, penetration length and occupied zone temperatures.

Lemaire [37], in simulations with the prescribed velocity inlet model found that for the higher flow rate cases (E2 and E3) the supply air jet dominates the flow pattern, causing a down-flow at the window. However, at the lowest flow rate (E1) the warm air rising from the window deflects the jet down from the ceiling. Flow instabilities were found at this condition which caused difficulties in achieving convergence to a steady-state solution. Simulations with the basic inlet model were easier to converge although some reduction in penetration length were observed.

Test case F (isothermal flow with contaminant)

Comparative data for the contaminant cases will be reported in the final Evaluation Report, to be completed prior to November 1991.

Test case 2D (isothermal flow and summer cooling)

Very detailed computations are possible for this particular test case, and useful data is coming forward. Some examples of the 2D test case results are shown in Figure 13. Generally good agreement is evident for velocities and turbulence quantities in iso-thermal flow. For non-isothermal flows both Chen [] and Lemaire [] have found strong hysteresis effects and difficulties in identifying an intermediate stage of jet projection.

Flow asymmetries

Evidence of flow asymmetries exists from the experimental data. In most simulations, however, a symmetry plane has been assumed, and so by definition no asymmetric flow patterns could be identified. However, some fine grid simulations have, under certain circumstances, been able to demonstrated flow asymmetries. Further analysis is required to identify the importance of this effect.

Case e2 PLANE K1

Air flow rate	: 0,0315 m^3/s	Air supply temperature	: 14,0 °C
Air change rate	: 3,0 1/h	Wall surface temperature	: 21,4 °C
Inlet velocity	: 3,32 m/s	Window surface temperature	: 30,2 °C

VELOCITIES

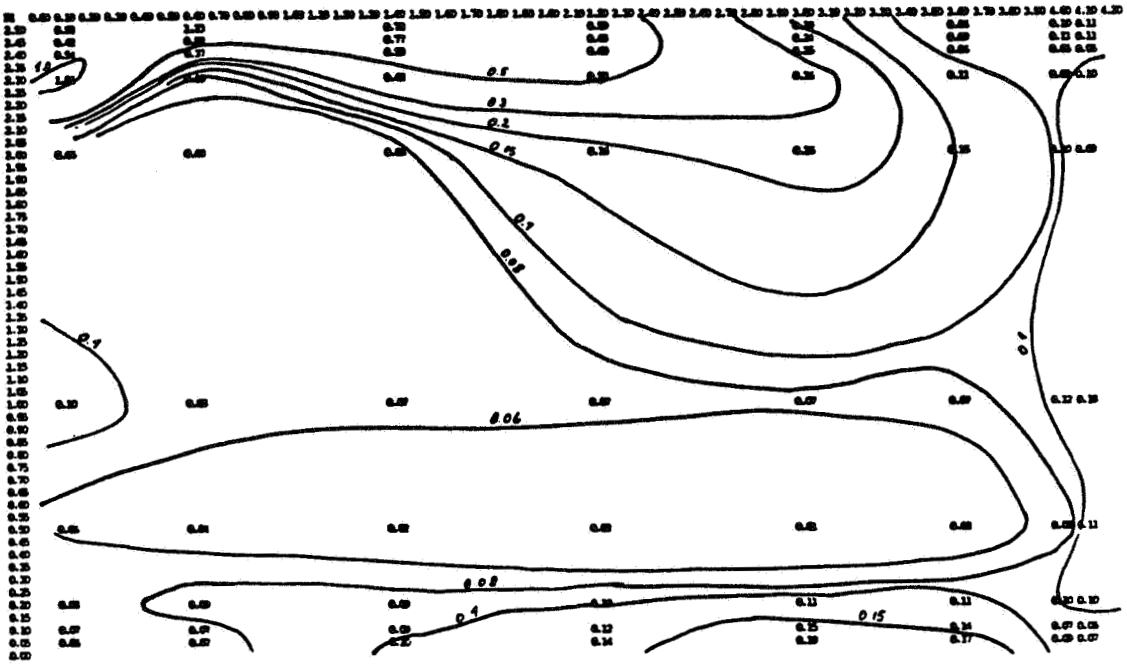

TEMPERATURES

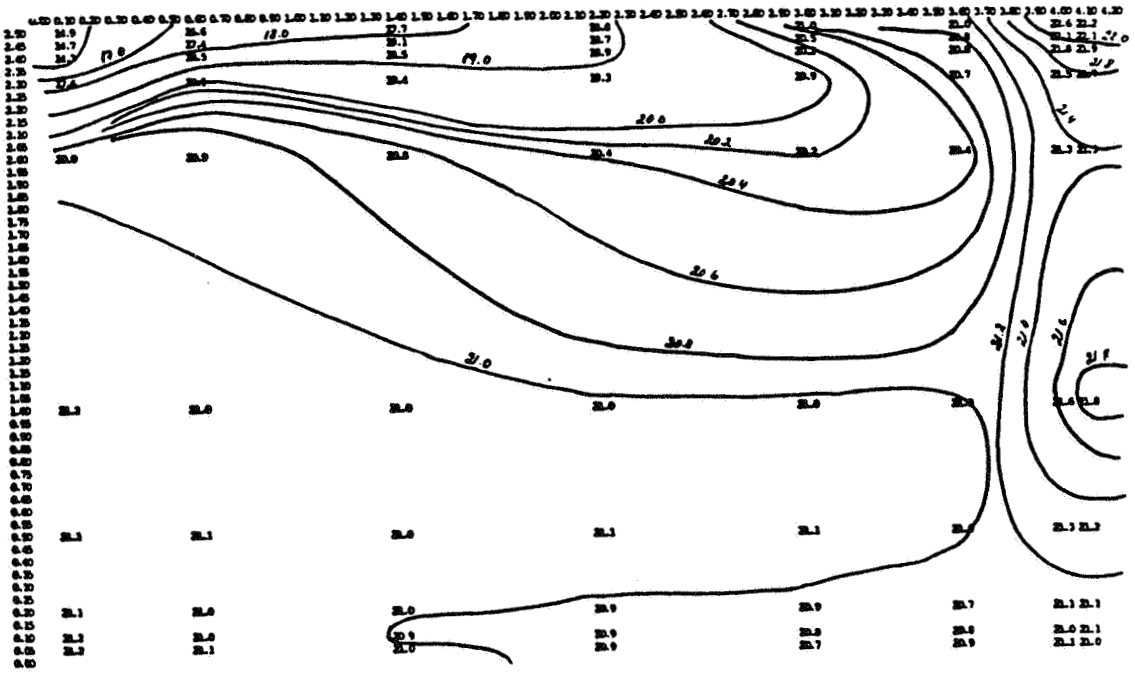

Figure 9 Measurement data for test case E2 (from Fossdal)

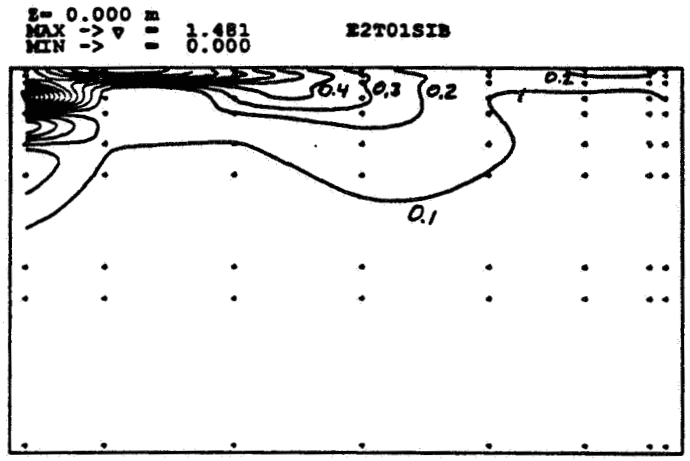

Isovels in plane z= 0.0 m

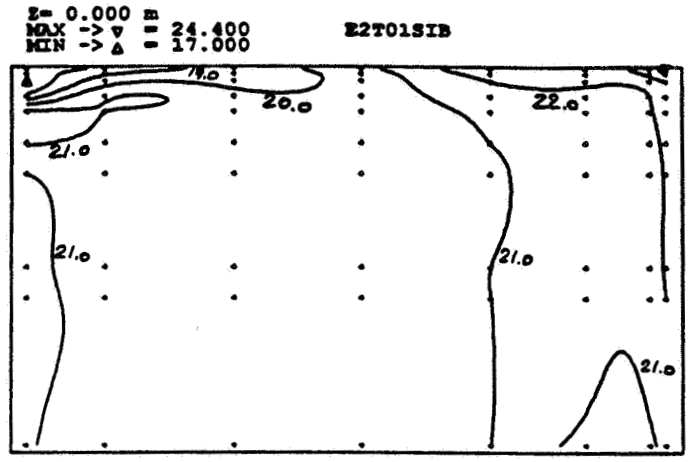

Isothermes in plane z= 0.0 m

Figure 10 Measurement data from test case E2
(from Blomqvist)

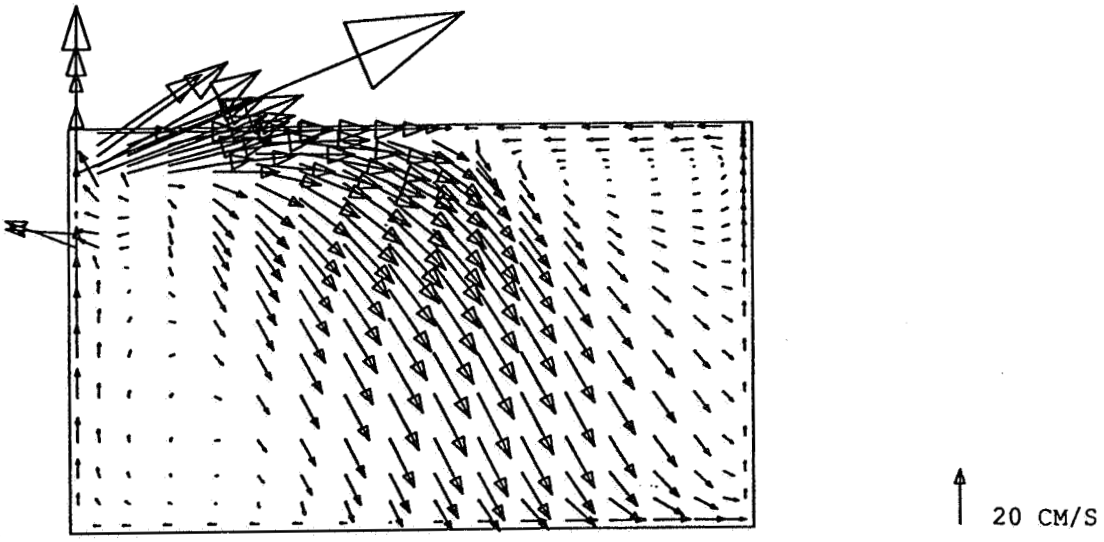

IEA Annex 20, Subtask 1, R.I. 1.20SF
Simulation case e1, plane k = 1 (symmetry plane)
Simulated velocity vectors

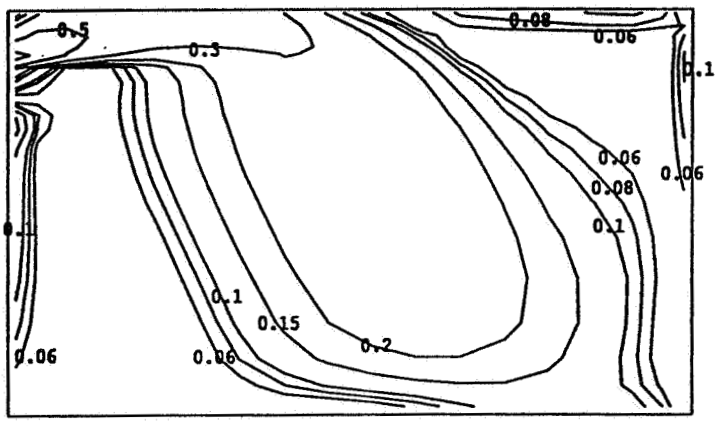

IEA Annex 20, Subtask 1, R.I. 1.20SF
Simulation case e1, plane k = 1 (symmetry plane)
Simulated contours of velocity (m/s)

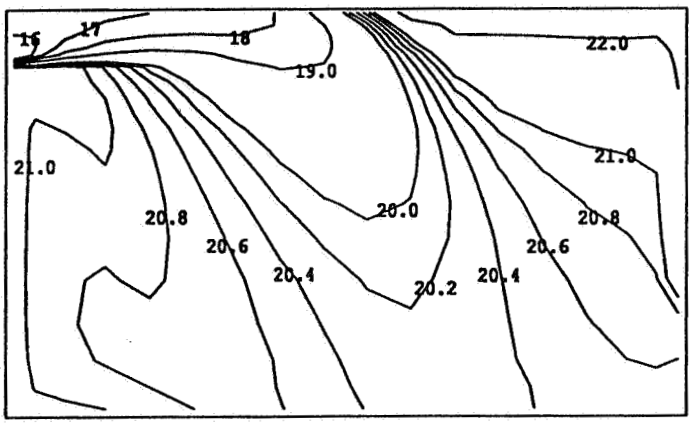

IEA Annex 20, Subtask 1, R.I. 1.20SF
Simulation case e1, plane k = 1 (symmetry plane)
Simulated contours of temperature (^{o}C)

Figure 11 Simulation data from test case E2 (from Heikkinen)

Table 8 Test case E1

Ref.	M or S	Ave. Um	Ave. Ut	Ave. U*	Max Um	Max Temp	Ave. Temp	Min Temp
E1FRG	S	0.029	0.040	0.052	0.112	18.90	18.56	18.10
E1CH	S	0.054	0.023	0.061	0.252	19.11	18.70	17.80
E1N	M	0.060	0.016	0.064	0.230	20.50	19.98	18.90
E1P001NL	S	0.060	0.031	0.069	0.266	20.09	19.81	19.07
E1CO2SF1	S	0.077	0.044	0.090	0.287	21.00	20.65	19.82
E1TO2SIB	M	0.087	0.039	0.096	0.234	21.80	20.85	20.00
E1GER	S	0.089	0.041	0.101	0.269	19.31	19.07	18.48

M= measured, S= simulated

Table 9 Test case E2

Ref.	M or S	Ave. Um	Ave. Ut	Ave. U*	Max Um	Max Temp	Ave. Temp	Min Temp
E2CD	S	0.015	0.005	0.019	0.056	20.00	20.00	19.99
E2FRG	S	0.049	0.052	0.074	0.085	19.40	19.15	19.10
E2FRGXQ	S	0.049	0.057	0.078	0.105	20.10	19.82	19.70
E2TO1SIB	M	0.066	0.034	0.075	0.181	22.00	21.19	20.50
E2N2	S	0.067	0.029	0.075	0.393	20.15	19.98	19.78
E2CH	S	0.068	0.038	0.080	0.279	19.50	19.18	18.50
E2B002NL	S	0.078	0.017	0.081	0.157	19.70	19.54	19.45
E2B001NL	S	0.078	0.019	0.081	0.167	19.46	19.35	19.26
E2N	M	0.083	0.021	0.086	0.260	21.40	20.95	20.20
E2P001NL	S	0.092	0.051	0.107	0.177	20.51	20.39	20.30
E2GER	S	0.096	0.048	0.109	0.181	19.75	19.63	19.46
E2CO1SF1	S	0.103	0.036	0.112	0.173	19.58	19.26	19.17
E2CO2SF1	S	0.108	0.048	0.122	0.194	21.09	20.75	20.60
E2T02SF1	M	0.123	0.036	0.129	0.260	21.35	20.86	20.28

Table 10 Test case E3

Ref.	M or S	Ave. Um	Ave. Ut	Ave. U*	Max Um	Max Temp	Ave. Temp	Min Temp
E3CH	S	0.092	0.051	0.109	0.172	19.50	19.24	19.07
E3FRG	S	0.121	0.100	0.163	0.217	19.40	19.06	18.90
E3N	M	0.152	0.030	0.155	0.350	21.20	20.51	20.10
E3GER	S	0.221	0.100	0.249	0.436	18.88	18.59	18.37
E3CO2SF1	S	0.231	0.065	0.243	0.417	20.21	19.83	19.53
E3P001NL	S	0.249	0.088	0.270	0.434	20.31	20.08	19.83
E3T02SF1	M	0.250	0.065	0.260	0.474	22.07	20.88	20.46

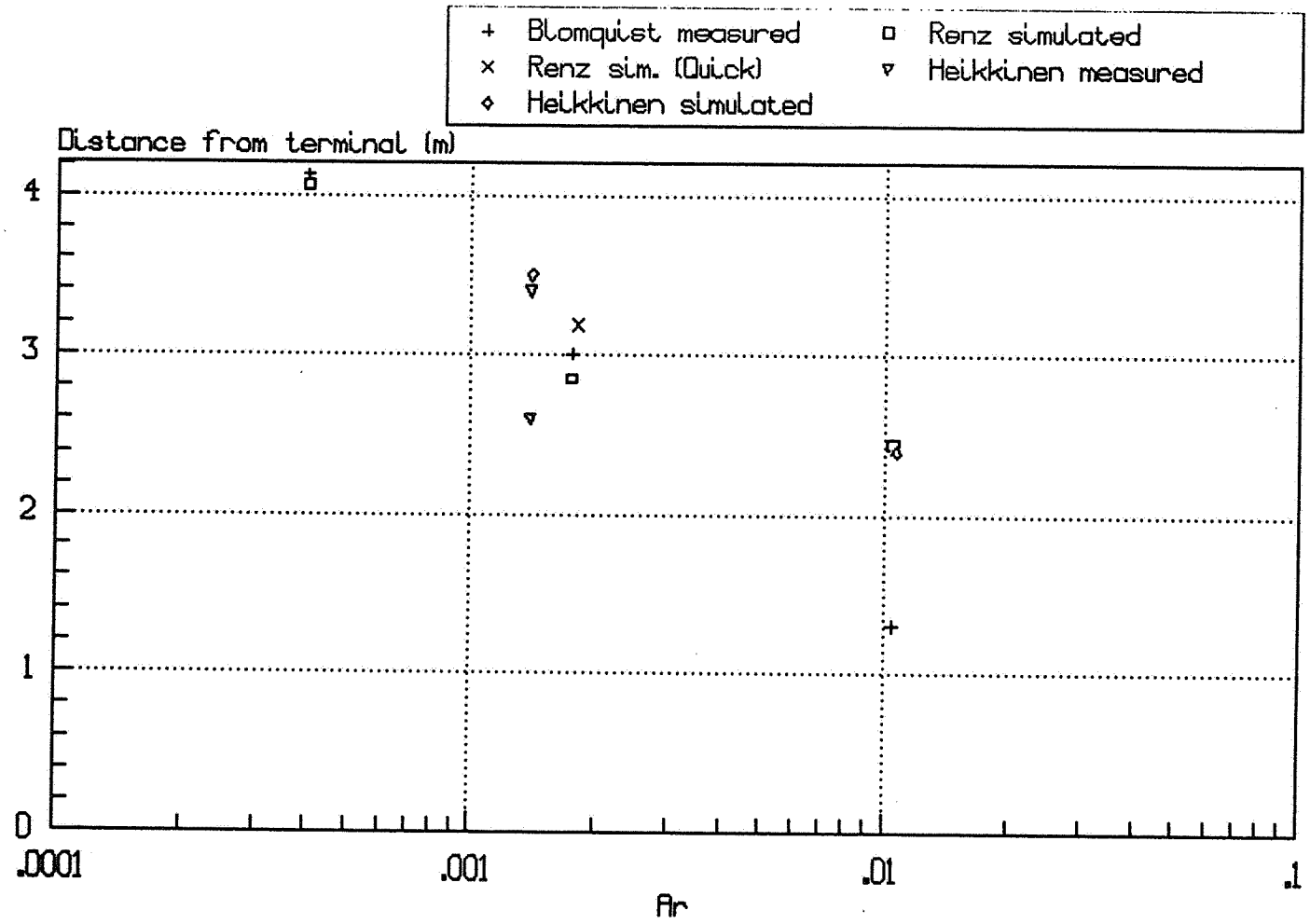

Figure 12 Penetration length of jet, test case E

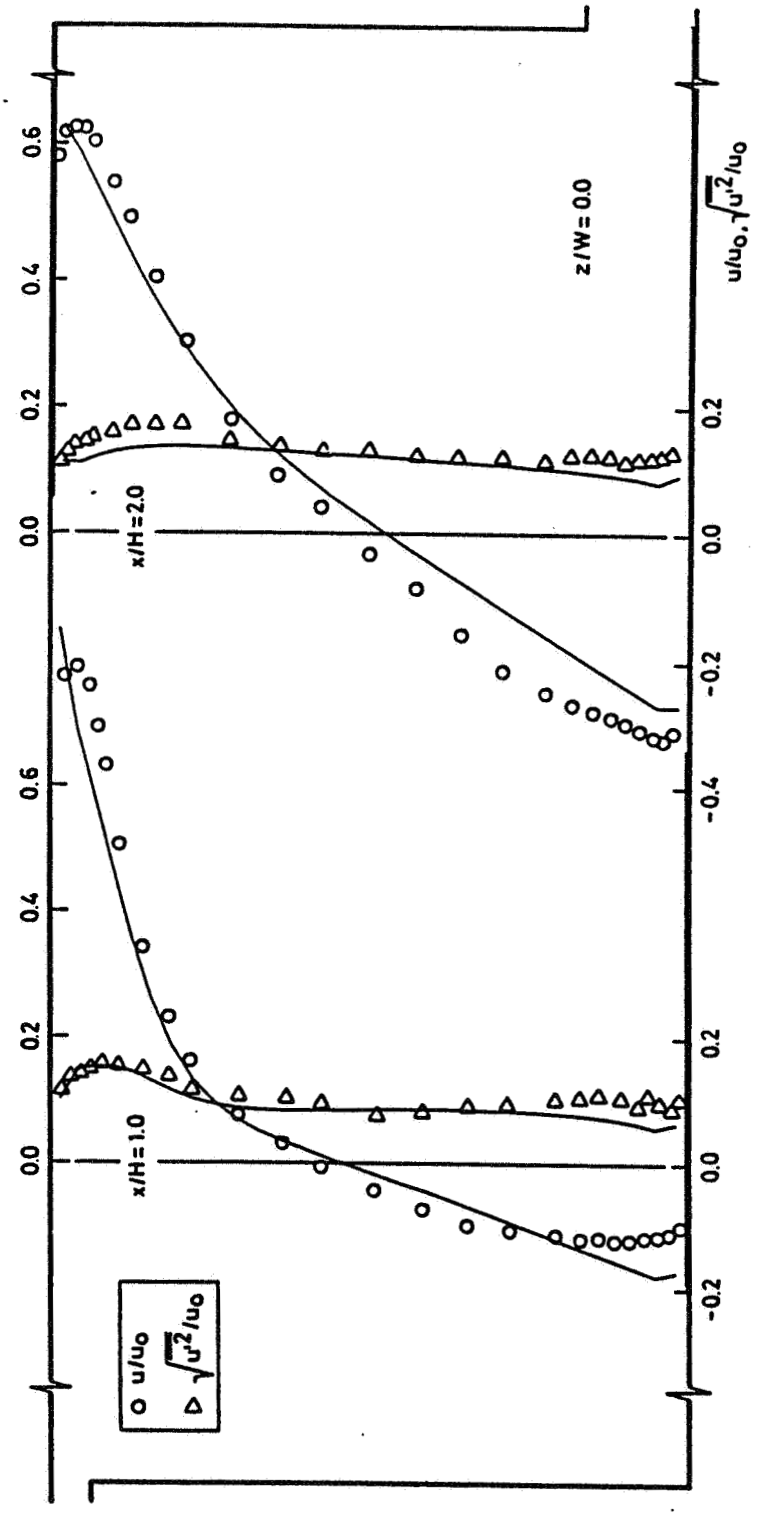

Comparison of measured and computed (solid-lines) mean and rms velocity.

Figure 13 Two dimensional simulation (isothermal) (from Lemaire)

Differencing scheme

The difference schemes used include Upwind, Hybrid, Power Law and Quick. Some indications are that higher order differencing schemes (eq. Quick) can be effective (Renz).

Grid refinement

A number of grid resolutions have been employed. Generally, the finer the grid the more accurate becomes the solution.

6. CONCLUDING REMARKS

The task of comparing and evaluating codes for room air movement prediction is an ambitious one. It is clear from the work already completed that difficulties exist, both associated with the computer predictions and in interpreting and rationalising real measurement data. The codes are difficult to use, time consuming and demanding in computer resources. Skill and experience are required to get the best from them. However, when used with care and, most importantly, with the exercise of sound engineering judgement it is clear that they can make a valuable contribution to understanding air movement in spaces and can predict room air movement with sufficient realism to be of use to design practice.

Some areas where further work is clearly needed, though, are:

- The modelling of the supply jet characteristics (which in these tests proved to be particularly difficult).

- Turbulence modelling. A range of results is found for predictions of turbulent velocity under similar conditions, particularly in buoyant flow. This can have implications for thermal comfort.

- Thermal wall functions. Temperature differences, in the occupied zone, from measurements and simulations are generally quite similar. But some simulations have identified serious shortcomings in predicting surface convection coefficients.

More detailed information on the findings of these studies can be found in participants' individual reports either listed in the References section at the end of this paper or about to be issued.

The project continues until 1 November 1991 and a more detailed written report must await the completion of the work.

8. ACKNOWLEDGEMENTS

The work reported here is based on measurements and computations carried out by many researchers. Table 11 lists those contributors and their organisations. The operating agent for Annex 20 is Dr. Alfred Moser, ETH Zurich, Switzerland, and the subtask 1 leader is Ir. Tony Lemaire, TNO, Delft, The Netherlands.

Table 11 Contributing investigators and organisations

Mr. Claes Blomquist	NSIBR, Gavle	SWEDEN
Mr. Jorma Heikkinen	VTT, Espoo	FINLAND
Dr. Qingyan Chen/ Dr. Alfred Moser	ETH, Zurich	SWITZERLAND
Mr. Michael Skovgaard/ Prof.Dr. Peter Nielsen	Univ. of Aalborg	DENMARK
Dr.-Ing. Johann Furst/ Mr. R Mohr	ROM, Hamburg	GERMANY
Ing. Tony Lemaire	TNO, Delft	NETHERLANDS
Prof.Dr.-Ing. Ulrich Renz/ Prof.Dr. Manfred Zeller/ Dipl.Ing. Markus Ewart	RWTH, Aachen	GERMANY
Dr. Christian Inard/ Dr. Francis Allard	INSA de Lyon	FRANCE
Ing. Didier Buty	CSTB, Marne la Vallee	FRANCE
Dr. Francis Biolley/ Dr. Jean-Raymond Fontaine	INRS, Vandoeuvre	FRANCE
Dr. M Nady Said	NRC, Ottawa	CANADA
Dr.Ing. Sverre Fossdal	NBRI, Oslo	NORWAY
Dr. Per Tjelflaat	SINTEF, Trondheim	NORWAY
Prof. Erik Olsson/ Dr. Lars Davidson	Chalmers Univ. of Tech., Goteborg	SWEDEN
Ing. Paolo Oliaro	Politecnico di Torino	ITALY

Financial support for the evaluation task is provided by the Building Research Establishment, Garston, Watford, UK.

7. REFERENCES

1. Patankar, S V. Numerical heat transfer, Hemisphere Pub., Washington DC, USA, 1980.

2. Baker, A J. Finite element computational fluid mechanics, Hemisphere Pub., Washington DC, USA, 1983.

3. ASHRAE Standard 55-1981. "Thermal Environmental Conditions for Human Occupancy", 1981.

4. ISO Standard 7730. "Moderate thermal environments - determination of the PMV and PPD indices and specification of the conditions for thermal comfort", 1985.

5. Anderson, D R., Sweeney, D J., and Williams, T A. Introduction to statistics - an applications approach. West publishing company. 1981.

6. Skovgaard, M., Hyldgaard, C E. and Nielsen, P V. High and low Reynolds number measurements in a room with an impinging isothermal jet, Proceedings of second international conference, ROOMVENT '90, Oslo, June 1990.

IEA Annex 20 Working Reports:

7. Heikkinen, J. Specification of testcase B (forced convection, isothermal). RID 1.13, April 1989.

8. Lemaire, A D. Specification of testcase D (free convection with radiator). RID 1.15, May 1989.

9. Heikkinen, J. Specification of testcase E (mixed convection, summer cooling). RID 1.14, April 1989.

10. Skaaret, Eimund. Specification of testcase F (forced convection, isothermal with contaminants). RID 1.31, Oct 1989.

11. Nielsen, P V. Specification of a two-dimensional test case. RID 1.45, Nov 1990.

12. Lemaire, A D. Testrooms, Identical testrooms. RID 1.03, May 1989.

13. Lemaire, A D. Selection of radiator. RID 1.04, April 1989.

14. Nielsen, P V. Selection of Air Terminal Device. RID 1.02, Dec. 1988.

15. Ruddick, K. and Whittle, G E. A proposed specification for a common data format. rid 1.22, May 1989.

16. Whittle, G E. and Ruddick, K. Proposal for data processing, evaluation and presentation. RID 1.22, November 1989.

17. Nielsen, P V. Representation of boundary conditions at supply openings. RID 1.11, February 1989.

18. Lemaire, A D. Modelling of boundary conditions near the radiator. RID 1.12, May 1989.

19. Heikkinen, J. Private communication.

20. Blomqvist, C. Measurement of test case B (forced convection, isothermal). AN20.1-S-91-SIB1, March 1991.

21. Heikkinen, J. Measurement results. May 1991.

22. Skovgaard, M. Simulation results. June 1991.

23. Moser, A., "Low Reynolds number effects in single room air flow". November 1988.

24. Chen Qingyan. Simulation of testcase B. January 1990.

25. Vogl, N. and Renz, U. Simulation of simple test cases. March 1991.

26. Lemaire, A D. Simulation of test case D (free convection with radiator), March 1991.

27. Inard, C and Buty, D. Simulation of test case D with zonal models. March 1991.

28. Blomqvist, C. Measurement results. June 1991.

29. Lemaire, A D. Measurement results for test case D2. July 1991.

30. Heikkinen, J. and Piira, K. Simulation of test case D (free convection with radiator) Preliminary Report. December 1990.

31. Renz, U. Simulation results. May 1991.

32. Fossdal, S. Measurement of test case E (mixed convection, summer cooling) Preliminary report. June 1990.

33. Blomqvist, C. Measurement of test case E (mixed convection, summer cooling). AN20.1-S-91-SIB2, March 1991.

34. Heikkinen, J. and Piira, K. Simulation of test case E (mixed convection, summer cooling) Preliminary Report. December 1990.

35. Ruddick, K R. and Whittle, G E. Presentation of Results from Measurements and Simulations of Test Cases B, E, and D, June 1990.

36. Whittle, G E. and Clancy, E. Presentation of Results from Measurements and Simulations of Test Cases B, D, and E, April 1991.

37. Lemaire, A D. Simulation of test case E (mixed convection , summer cooling), March 1991.

38. Chen Qingyan. Simulation of simple test cases. RID 1.46, March 1991.

39. Lemaire, A D. Simulation of simple test cases 2D1, 2D2. May 1991.